1-1-2014

Influence of pallets on the behaviour and design of steel drive-in racks

Benoit Gilbert
Griffith University, b.gilbert@griffith.edu.au

Lip H. Teh
University of Wollongong, lteh@uow.edu.au

Romain X. Badet
Griffith University

Kim Rasmussen
The University of Sydney, k.rasmussen@usyd.edu.au

Influence of pallets on the behaviour and design of steel drive-in racks

Abstract

This paper analyses the influence of horizontal bracing restraints provided by the friction between pallet bases and rail beams on the static behaviour and design of steel drive-in storage racks. The pallet bracing restraints are shown to significantly influence the structural behaviour of the rack, and their effect on the bending moment distribution of the uprights is studied in the paper. The 2D single upright model proposed by Godley is improved in this study by including the restraints provided by the plan flexural stiffness of the rail beams and the friction between the pallets and rail beams. The improved 2D model was found to accurately reproduce the bending moment distributions obtained using 3D advanced finite element analysis. The 2D single upright model is used to analyse 36 drive-in racks under various load case combinations. The paper evaluates the influence of the pallet bracing restraints on the ultimate capacity of drive-in racks, clarifies the loading pattern(s) governing the structural design and determines the friction coefficient, or strength of a restraining device, required to prevent the pallets from sliding. It is shown that while restraints from pallets could potentially be considered in design, they would not lead to more economic structural solutions.

Keywords

behaviour, design, steel, influence, drive, pallets, racks

Disciplines

Engineering | Science and Technology Studies

Publication Details

Gilbert, B. P., Teh, L. H., Badet, R. X. & Rasmussen, K. (2014). Influence of pallets on the behaviour and design of steel drive-in racks. Journal of Constructional Steel Research, 97 10-23.

INFLUENCE OF PALLETS ON THE BEHAVIOUR AND DESIGN OF STEEL DRIVE-IN RACKS

Benoit P. Gilbert[(1)], Lip H. Teh[(2)], Romain X. Badet[(3)], Kim J.R. Rasmussen[(4)]

[(1)] Senior Lecturer, Griffith School of Engineering, Griffith University, Australia
[(2)] Senior lecturer, School of Civil, Mining and Environmental Engineering, University of Wollongong, Australia
[(3)] Former exchange undergraduate student, Griffith School of Engineering, Griffith University, Australia
[(4)] Professor, School of Civil Engineering, University of Sydney, Australia

ABSTRACT

This paper analyses the influence of horizontal bracing restraints provided by the friction between pallet bases and rail beams on the static behaviour and design of steel drive-in storage racks. The pallet bracing restraints are shown to significantly influence the structural behaviour of the rack, and their effect on the bending moment distribution of the uprights is studied in the paper. The 2D single upright model proposed by Godley is improved in this study by including the restraints provided by the plan flexural stiffness of the rail beams and the friction between the pallets and rail beams. The improved 2D model was found to accurately reproduce the bending moment distributions obtained using 3D advanced finite element analysis. The 2D single upright model is used to analyse 36 drive-in racks under various load case combinations. The paper evaluates the influence of the pallet bracing restraints on the ultimate capacity of drive-in racks, clarifies the loading pattern(s) governing the structural design and determines the friction coefficient, or strength of a restraining device, required to prevent the pallets from sliding. It is shown that while restraints from pallets could potentially be considered in design, they would not lead to more economic structural solutions.

KEYWORDS

Steel drive-in racks, steel storage racks, steel structures, pallet bracing restraints.

NOTATIONS

Symbol		Designation
A_u	=	Cross-sectional area of upright members
C_b	=	Coefficient depending on the BMD in the unbraced segment
E	=	Steel Young's modulus
f	=	Out-of-plumb load applied to a rail beam
$f_{u,m}$	=	Load applied in the translational stiffness $K_{uh,m}$
f_{oy}, f_{oz}	=	Elastic buckling stresses about the y- and z- axes
h, h_p	=	Frame bracing pitch
h_{rail}	=	Rail beam elevation
H	=	Height of the rack
I_u	=	Second moment of area of the upright
I_r	=	Second moment of area of two rail beams
k_u	=	Upright stiffness
K_b	=	Top rotational stiffness of the upright for a rack is sway mode
K_c	=	Base plate rotational stiffness of the base plate to floor connection
$K_{r,i}$	=	Rail beam translation stiffness at rail beam elevation i
K_t	=	Top translational stiffness for the single upright model
K_{uh}	=	Horizontal translational stiffness of the upright at the point of application of load P
$K_{uh,m}$	=	Horizontal translational stiffness of the inner uprights
$K_{uh,fb}$	=	Horizontal translational stiffness of the front and back uprights
l_{ex}, l_{ey}, l_{ez}	=	Effective buckling lengths about the x-, y- and z- axes, respectively
L	=	Distance between two uprights (upright frame width)
N^*	=	Design factored axial load
N_c	=	Nominal axial compression capacity of the upright
N_{cd}	=	Nominal axial compression distortional capacity of the upright
N_{cl}	=	Nominal axial compression local capacity of the upright
N_{ce}	=	Nominal axial compression global capacity of the upright
N_{crb}	=	Elastic buckling load of the upright determined from an elastic buckling analysis
N_s	=	Number of rail beam elevations
N_u	=	Number of uprights in the down-aisle direction
M_{bx} ,M_{by}	=	Nominal bending moments capacity of the upright about the x- and y-axes, respectively
M_{bxd}	=	Nominal distortional bending moment capacity of the upright about the x-axis
M_{bxl}	=	Nominal local bending moment capacity of the upright about the x-axis
M_{bxe}	=	Nominal global bending moment capacity of the upright about the x-axis
M_o	=	Global buckling moment
M_x^*, M_y^*	=	Design factored bending moments about the x- and y-axes, respectively
P	=	Horizontal load applied to the upright
P_b, P_c	=	Load
s	=	Friction effect
S_f	=	Friction force
r_{ol}	=	Radius of gyration
W	=	Pallet load
α	=	Out-of-plumb angle
Δ	=	Total down-aisle displacement at the top of a drive-in rack
Φ_b	=	Reduction capacity factor for member in bending
Φ_c	=	Reduction capacity factor for member in compression
ω	=	Pallet uniform distributed load
μ	=	Friction coefficient

1 INTRODUCTION

Worldwide, steel storage racks are extensively used in the manufacturing, wholesale and retail industry to store goods. They are mostly freestanding structures and are often assembled from cold-formed steel profiles. Two main types of racks prevail, referred to as “selective racks” and “drive-in racks”. In drive-in racks, pallets are stored on rail beams one after the other, and the forklift truck drives into the rack to store the pallets on the “first-in last-out” principle. The rail beams are offset from the centreline of the uprights so that the pallets apply both bending moments and axial compressive forces to the uprights. To allow the forklift truck passage, the rack is only braced horizontally at the top (plan bracing) and vertically at the back (spine bracing) in the down-aisle direction. Due to their floor space efficiency, drive-in racks are usually preferred to selective racks when storing the same goods with quick turnover, or in expensive storage spaces such as industrial freezers. Figure 1 shows an example of a drive-in rack.

Experimental tests performed by Gilbert and Rasmussen [1] have shown that pallets act as horizontal braces between adjacent uprights, significantly influence the structural behaviour of drive-in racks and must be considered in order to accurately capture the 3D behaviour of drive-in racks. Similarly, earlier research by Salmon et. al. [2], who numerically investigated the buckling behaviour of symmetrically loaded drive-in racks by alternately considering and ignoring the pallet bracing restraints in the analysis, showed that pallet bracing restraints had significant influence on the non-sway buckling mode, although they had less influence on the sway buckling mode.

However, due to the uncertainty concerning the friction between the pallet bases and the rail beams, drive-in racks are currently designed without considering the bracing effects. If a device can prevent the pallets from sliding on the rail beams or if the coefficient of friction between the pallet bases and the rail beams can be reliably determined, the horizontal bracing effect provided by the pallets could be fully exploited in the design of a drive-in rack.

Hua and Rasmussen [3] measured the friction coefficient between wood pallets and rail beams and found that the average static friction coefficient between the rail beams and the pallet bases to be as high as 0.576, with a recommended design static friction coefficient of 0.439. This friction coefficient suggests that significant horizontal forces can develop between the pallets and the rail

beams before sliding occurs, allowing the pallets to play a structural role in the behaviour of drive-in racks. It is noted, however, that this design static friction coefficient does not take into account grease or ice (in the case of industrial freezers) that may accumulate on rail beams.

Another aspect related to pallet bracing restraints is the in-plane shear stiffness of the pallet base. Hua and Rasmussen [3] experimentally found that the in-plane shear stiffness of pallet bases ranged from 5.1 N/mm to 31.4 N/mm, depending on the pallet condition. Characteristic design shear stiffness values of 3.9 N/mm for pallets deemed in poor condition and 8.3 N/mm for pallets deemed in good condition were recommended.

The current paper analyses the influence of the horizontal bracing effect of pallets on the static behaviour and design of steel drive-in racks in the down-aisle direction only, as due to the upright frames, pallets are not believed to influence the behaviour of drive-in racks in the cross-aisle direction. It should also be noted that the friction between pallet bases and the rail beams would prevent the pallets from dropping through on account of the upright bowing deformations [4, 5]. As such, the serviceability check against upright bowing deformations is not considered in this paper.

The 2D analysis model for drive-in racks proposed by Godley [6] is improved herein by introducing the horizontal restraints provided by both the rail beams and the pallet bracing restraints. The improved model is checked against the 3D model developed by Gilbert and Rasmussen [1, 7] that is calibrated against laboratory test results. The influence of the pallet restraints on the bending moment distribution in the uprights is also evaluated. Thirty six drive-in racks representing the global sale of an Australian manufacturer over three years are then analysed using the improved 2D model under all possible static loading scenarios, alternately considering and ignoring the pallet bracing restraints. This paper evaluates the influence of pallet bracing restraints on the ultimate capacity of steel drive-in racks in the down-aisle direction, clarifies the loading scenario(s) governing the design and determines the friction coefficient or the strength of a restraining device required to prevent the pallets from sliding.

2 SINGLE UPRIGHT MODEL

2.1 Single upright model proposed by Godley

In order to reduce the computation time associated with large models, Godley [6] developed a "single upright model" to analyse fully loaded drive-in racks in the down-aisle direction. The upright is restrained at its base by a spring support having a rotational stiffness K_c, and at its top by another having a rotational stiffness K_b and a translational stiffness K_t, as shown in Figure 2. K_c represents the restraint provided by the base plate to the floor connection, K_b the restraint provided by the portal beams in double curvature (sway mode) having semi-rigid connections to the upright, and K_t the combined restraint from the plan bracing (spanning the entire rack), spine bracing (spaning one bay) and upright frames. Pallet loads and out-of-plumb loads are applied to the upright as shown in Figure 2, where the rack is assumed to be fully loaded such that loads W are applied on all rail beams. Detailed calculations for K_c, K_b and K_t, can be found in [6].

Despite its attractiveness, this model has limitations as it (i) ignores the restraint provided by the rail beams, (ii) does not take into account the horizontal bracing restraint provided by pallets, and (iii) does not consider all possible upright loading scenarios, including partially loaded racks where pallet loads are placed asymmetrically so as to induce bending of the upright. These limitations are addressed in following sections.

2.2 Improved single upright model

2.2.1 Rail beam restraints

Typically, the out-of-plumb of drive-in racks is modelled by horizontal forces at the rail beam supports that are linearly proportional to the gravity loads of the pallets (see section 4.1.2). For a fully loaded rail beam, the front and the back uprights are less loaded than the inner uprights, resulting in smaller out-of-plumb forces being applied to the front and back uprights, as illustrated in Figure 3 for a rack with two upright frames. Therefore and since rail beams link the uprights together, they restrain the deflection of the inner uprights when subjected to the out-of-plumb forces, as shown in Figure 3 (b), in which α is the out-of-plumb angle with vertical.

Consequently, these restraints provided by the rail beams are introduced into the single upright model by adding a horizontal translational stiffness $K_{r,i}$ at each rail beam elevation i, as shown in Figure 4. An expression for $K_{r,i}$ is derived in Section 2.2.1.2.

2.2.1.1 Upright down-aisle stiffness K_{uh}

Consider an upright of height H and second moment of area I_u that is subjected to a down-aisle force P at a distance h_{rail} from the floor, as shown in Figure 5 (a). The upright is restrained at its base by the rotational stiffness K_c provided by the base plate to floor connection, and at its top by the rotational stiffness K_b provided by the upright to portal beam connection. The total deformation of the upright can be resolved into three distinct parts with various boundary conditions and applied loads, as illustrated in Figure 5 (b-d), and the down-aisle stiffness K_{uh} of the upright (Figure 5 (e) is then given as [8],

$$\frac{1}{K_{uh}} == \frac{h_{rail}^3(H-h_{rail})}{3EI_uH^2}\left[\left(K_c\left(1-\frac{h_{rail}}{3H}\right)+2k_u\frac{H}{h_{rail}}\right)\frac{1}{P_c}+\frac{h_{rail}K_b}{3HP_b}-\frac{H}{3}\right] \tag{1}$$

where

$$\frac{1}{P_c}=\frac{(4k_u+K_b)(H-h_{rail})+2k_uh_{rail}}{12k_u^2+4k_u(K_c+K_b)+K_cK_b} \tag{2}$$

$$\frac{1}{P_b}=\frac{(4k_u+K_c)h_{rail}+2k_u(H-h_{rail})}{12k_u^2+4k_u(K_c+K_b)+K_cK_b} \tag{3}$$

and

$$k_u=\frac{EI_u}{H} \tag{4}$$

2.2.1.2 Upright down-aisle stiffness $K_{r,i}$

The stiffness $K_{r,i}$ is derived herein for the critical upright (second from the front) of a drive-in rack with two upright frames and uniform spacing between uprights. For simplicity, the restraints provided by all rail beams to an upright are assumed to be independent of each other.

Each rail beam is restrained at its supports by the upright down-aisle stiffness K_{uh}, derived in Section 2.2.1.1. Since the base plate to floor connection stiffness K_c depends on the axial load in

the upright [9] and the front and back uprights are less loaded than the inner uprights, the upright down-aisle stiffness K_{uh} varies accordingly. This variation is represented in Figure 6 with the rail beam restrained at the front and back uprights by spring supports each having the stiffness $K_{uh,fb}$ and at the inner uprights by springs having the stiffness $K_{uh,m}$.

The force $f_{u,m}$ in the inner springs in Figure 6 can be expressed as [8],

$$f_{u,m} = f\frac{\frac{11L^3}{12EI_r}+\frac{3}{2K_{uh,fb}}}{\frac{5L^3}{6EI_r}+\frac{1}{K_{uh,fb}}+\frac{1}{K_{uh,m}}} \tag{5}$$

where $3f$ is the total out-of-plumb force applied to the rail beam (see Figure 3 (b) and Figure 6), L is the distance between two uprights and I_r is twice the second moment of area of the rail beam, as two rail beams are typically connected to the uprights.

Replacing the rail beam in Figure 6 with its equivalent stiffness $K_{r,i}$ at the critical upright (either point B or C), using static equilibrium and the expression for $f_{u,m}$ in Eq. (5), the translational restraint $K_{r,i}$ provided by the rail beam to the upright at the i^{th} beam level is then expressed as [8],

$$K_{r,i} = \frac{11K_{uh,fb}-4K_{uh,m}}{\frac{55L^3K_{uh,fb}}{6EI_r}+15} \tag{6}$$

2.2.2 Pallet bracing restraints

The bracing effect provided by the pallets is now considered for any loading scenario of a studied single upright. Bays not directly in the vicinity of this upright are assumed to be fully loaded, as it would maximise the down-aisle displacement Δ of the rack and therefore the P-Δ effects in the upright. Specifically, two loading scenarios are considered for these bays, believed to represent the two design envelopes:

- Bay loading scenario A: all bays not directly connected to the studied upright are fully loaded, as shown in Figure 7 (a).
- Bay loading scenario B: the two bays on each side of the two bays directed connected to the studied upright are empty, while the remaining bays are fully loaded, as shown in Figure 7 (b). This loading scenario aims to limit the influence of the pallets on the bending moment distribution in the

studied upright, since contrary to the previous Bay loading scenario A, the pallets only link the studied upright and its two neighbours.

2.2.2.1 Improved model for Bay loading scenario A (Model A)

In a fully loaded rack, the influence of the pallets on the deformed shape of the uprights would be minimal, as all internal uprights in a row of uprights in the down-aisle direction would identically deform. Therefore, the overall deformation of the rack at the critical row of uprights can be found using the fully loaded improved single upright model introduced in Section 2.2.1, i.e. not considering pallets, as illustrated in Figure 8. Moreover, if the number of bays of the rack is large, as frequently encountered in drive-in racks (see Figure 1), removing pallets from each side of the studied upright would have negligible influence on the overall deformation of the rack, and the deformation of this upright would be a function of both its immediate loading configuration and the overall deformation of the rack imposed to the upright by the portal beams and the pallet bracing restraints.

Therefore, the bracing restraint provided by the pallets for a given loading scenario of the single upright is introduced into the model in the following manner, as illustrated in Figure 9:

Step 1: The overall down-aisle displacements of the rack at each rail beam elevation and at the top of the rack are determined using the fully loaded single upright model with out-of-plumb forces, as shown in Figure 8. The base plate to floor rotational stiffness K_c, and rail beam stiffness $K_{r,i}$ are calculated for the fully loaded configuration.

Step 2: The single upright model is loaded with its studied loading scenario, with the corresponding base plate to floor rotational stiffness K_c and rail beam stiffness $K_{r,l}$, determined for the axial load in the studied upright.

Step 3: The overall down-aisle displacement at the top of the rack (portal beam elevation) found in Step 1 is imposed at the top of the single upright model created in Step 2.

Step 4: For each rail beam elevation of the model in Step 2, if there is at least one pallet at the elevation, then the overall down-aisle displacement at that elevation found in Step 1 is imposed on the upright.

2.2.2.2 Improved model for Bay loading scenario B (Model B)

In order to determine the bending moment distribution in the studied upright for a given loading scenario of the upright, three single upright models are used and linked together by pinned rigid elements (ties) representing the pallet bracing restraints. The following steps are carried out as illustrated in Figure 10:

Step 1: As with the previous Bay loading scenario A, the overall displacement imposed by the rack at the top of the critical upright and its two adjacent uprights (Figure 7 (b)) is determined using the fully loaded single upright model with out-of-plumb forces, as shown in Figure 8. The base plate to floor rotational stiffness K_c, and rail beam stiffness $K_{r,i}$ are calculated for the fully loaded configuration.

Step 2: A three single upright model is created and loaded with the studied loading scenario. The base plate to floor rotational stiffness K_c and rail beam stiffness $K_{r,i}$ for each of the three uprights is determined separately for the axial load in the upright.

Step 3: The overall down-aisle displacement at the top of the rack (portal beam elevation) found in Step 1 is imposed at the top of the three uprights created in Step 2.

Step 4: Pallet bracing restraints are modelled using horizontal ties between rail beams, as shown in Figure 10.

3 INFLUENCE OF THE PALLET RESTRAINT ON THE BENDING MOMENT DISTRIBUTION AND VALIDATION OF THE SINGLE UPRIGHT MODEL

The 3D advanced Finite Element model for drive-in racks developed by Gilbert and Rasmussen [1, 7] is used herein to (i) analyse the influence of the pallet restraint on the bending moment distribution in the upright and (ii) validate the improved single upright model introduced in Section 2.2. The 3D model has been calibrated against experimental test results and considers joint eccentricities, nonlinear portal beam-to-upright connections, nonlinear base-plate connections, and pallet bracing restraints. Seven degrees of freedom (i.e. Warping considered) beam elements are used in the 3D Finite Element model. Refer to [1, 7] for more details. In the present 3D second-order analysis, the FE software Abaqus [10] is used, while the FE software Strand7 [11] is used to

run the 2D second-order analysis of the improved single upright model. It may be noted that while the 2D model ignores torsion and warping of the uprights (phenomena that are considered in the 3D model), it closely predicts the overall down-aisle behaviour of the rack, as developed using the 3D model in Sections 3.1 and 3.2. Therefore, torsion and warping of the uprights are likely have a limited influence on the overall drive-in rack behaviour.

A rack with similar characteristics to the one tested by Gilbert and Rasmussen [1] is used as a case study in this validation. Specifically, the rack is 12 bays wide, 4 pallets and 2 upright frames deep, and 4 stories high (i.e. featuring 3 rail beam levels). It has 3 spine bracing modules, each spanning one bay, and 4 plan bracing modules, each spanning three bays. The overall lay-out of the rack is shown in Figure 11. Each pallet load is 2 tonnes. The rack is loaded as in Bay loading scenario A, described in Section 2.2.2. The shear stiffness of the pallets is taken as 7.2 N/mm, which is within the range experimentally found by Hua and Rasmussen [3]. The pallets are considered to be fastened to the rail beams as the static friction coefficient is assumed to be sufficiently high to prevent sliding. Two loading scenarios are studied, with the out-of-plumb and other design parameters given in Section 4.1. Further verification of the improved single upright model can be found in [8].

3.1 First loading scenario – Maximum combined axial compression and bending

The load case involving the loading scenario shown in elevation in Figure 12 generally represents the governing load case for combined axial compression and bending of the critical upright adjacent to the unloaded compartment and to the aisle upright [12].

The down-aisle bending moment distribution of the critical upright from the 3D model accounting for pallet bracing restraints is plotted in Figure 13 (a), and that obtained from the 3D model ignoring pallet bracing restraints in Figure 13 (b). Figure 13 shows that the pallet bracing restraints significantly affect the bending moment distribution of the critical upright, but have only a relatively minor impact on the maximum design bending moment. This observation appears to be general for this type of loading scenario. Note, however, that depending on the rack configuration, the design moment in the critical section of the upright may be larger when pallet restraints are considered, and

hence lower capacities may, in fact, result from considering pallet restraints compared to ignoring pallet restraints. This unexpected result is investigated further in Section 5.1.1.

The down-aisle bending moment distribution of the critical obtained from the single upright model accounting for pallet bracing restraints described in Section 2.2.2.1 is plotted in Figure 14(a), and that obtained from the single upright model ignoring pallet bracing restraints (i.e. ignoring Step 4 in Section 2.2.2.1) in Figure 14 (b). It can be seen from the comparison between Figure 13 and Figure 14 that the single model upright is able to accurately reproduce the bending moment distribution of the critical upright, with and without pallet bracing restraints. The difference in the design bending moment between the 3D and the single upright models is less than 6%.

3.2 Second loading scenario – Maximum bending

The load case involving the loading scenario shown in Figure 15 typically induces the largest design bending moment in the critical upright. The down-aisle bending moment distribution of the critical upright under the second load case obtained from the 3D model accounting for pallet bracing restraints is plotted in Figure 16 (a), and that obtained from the 3D model ignoring pallet bracing restraints in Figure 16 (b). Figure 16 shows that the pallet bracing restraints not only significantly affect the bending moment distribution of the critical upright, but also reduce the maximum design bending moment by almost one third under the second load case.

The down-aisle bending moment distribution of the critical upright obtained from the single upright model accounting for pallet bracing restraints is plotted in Figure 17 (a), and that obtained from the single upright model ignoring pallet bracing restraints in Figure 17 (b). Consistent with the results for the previous loading scenario, the comparison between Figure 16 and Figure 17 shows that the single model upright is able to accurately reproduce the bending moment distribution of the critical upright, with and without pallet bracing restraints. The difference in the design bending moment between the 3D and the single upright models is less than 7%.

4 PARAMETRIC STUDIES

Thirty-six rack configurations, representing the global sale of an Australian manufacturer over three years and designed using industry practice [12], are analysed using the single upright models. The racks are considered to be 4 pallets deep, with rail beams equally spaced along the rack height. The uprights are referred to as “SD” for standard uprights and “RF” for rear flanged uprights, their widths range from 70 mm to 150 mm and their thicknesses from 1.2 mm to 2.4 mm. Table 1 summarises the rack configurations including the rack height, design pallet load, number of storeys and upright type. More details can be found in [8, 13].

Specifically, three different single upright models are considered and their member action-to-capacity ratios are used to quantify the influence of pallet restraints on the design of drive-in racks:

- Model A considers the pallet bracing restraints and represents the Bay loading scenario A. The model is described in Section 2.2.2.1 and illustrated in Figure 9.
- Model B considers the pallet bracing restraints and represents the Bay loading scenario B. The model is described in Section 2.2.2.2 and illustrated in Figure 10.
- Model C is based on the current industry practice of neglecting pallet bracing restraints. The model is similar to Model A with the exception of Step 4 in Section 2.2.2.1.

4.1 Design parameters

4.1.1 Base plate to floor connection stiffness

Base plates are generally bolted to the floor, and the strength and initial rotational stiffness of the base plate to floor connection depend on the axial load in the upright [9]. Numerical investigations on the non-linear behaviour of a typical storage rack base plate assembly [14] showed that (i) the connection strength is proportional to the upright width, (ii) in the presence of axial load in the upright, the initial rotational stiffness of the base plate to floor connection is proportional to the cube of the upright width and (iii) when no axial load is applied to the upright, the initial rotational stiffness is independent of the upright width.

The rules described above, combined with the test results in [14] applicable to a 125 mm wide base plate assembly, are used in the following sections to determine the initial stiffness and strength

of base plate to floor connections as functions of base plate width. The detailed moment-rotation curves used in the present work are given in [8].

4.1.2 Out-of-plumb

The main international racking specifications [15-17] consider the initial looseness in the member connections as well as the initial out-of-plumb as frame imperfections, which are generally accounted for in the design by means of horizontal forces $F_{out\text{-}of\text{-}plumb}$ applied at each rail beam elevation as,

$$F_{out-of-plumb} = \alpha W \tag{7}$$

where α is the out-of-plumb angle and W is the vertical load applied to the upright by the pallets at the rail beam elevation. The out-of-plumb angle α is typically a function of the number of interconnected bays and the looseness in the portal beam to upright connections. A typical out-of-plumb angle of 0.0044 rad (about 1/250) is used in the present work, see [8] for more details.

4.1.3 Other parameters

Other design parameters used in the present work, which correspond to drive-in rack configurations currently commercialised in Australia, are given in [8]. The height of the rack H, the number of pallet levels N_s and the cross-sectional area of the upright A_u depend on the studied rack characteristics and are given in Table 1 and [8].

4.2 Upright load cases

According to the FEM specification for the design of drive-in racks [12], the load case involving the loading scenario depicted in Figure 12 and a fully loaded upright are usually “sufficient to consider the pattern load effects” for the Ultimate Limit State (ULS) design in the down-aisle direction. However, it is currently unclear if a different load case may govern the design. Moreover, in light of the horizontal bracing effect offered by the pallets, the load case involving the loading scenario depicted in Figure 12 and a fully loaded upright may not always be sufficient for the ULS design of the upright.

Consequently, every possible load case is investigated in the present work for the 36 drive-in racks given in Table 1. Similar to Section 3, second-order geometric analyses are carried out using the general purpose FE software Strand7 [11]. The number of load cases analysed per rack is a function of the number of rail beams and is equal to 4^{Ns}, where N_s is the number of rail beam elevations.

4.3 Ultimate capacity

For each of the three rack models (A, B, C) and each upright load case, the Australasian/New Zealand cold-formed steel structures standard AS/NZS 4600 [18] is used to calculate the member action-to-capacity ratios of the critical upright. When second order-geometric analyses are used, members subjected to combined axial compression and bending must satisfy the ULS design check in Eq. (8),

$$\frac{N^*}{\phi_c N_c} + \frac{M_x^*}{\phi_b M_{bx}} + \frac{M_y^*}{\phi_b M_{by}} \leq 1 \tag{8}$$

where N^* is the design axial compression load, and M_x^* and M_y^* are the design bending moments about the x- (cross-aisle) and y- (down-aisle) axes (see Figure 11 (c) for axes details), respectively, N_c is the nominal axial compression member capacity, M_{bx} and M_{by} are the nominal member bending moment capacities about the x- and y- axes, respectively, ϕ_c and ϕ_b are reduction capacity factors for members in compression and bending, taken as 0.85 and 0.90, respectively. As the present work is concerned with the design of drive-in racks in the down-aisle direction, the bending moment about the down-aisle axis is considered negligible and for the 2D single upright model, Eq. (8) becomes,

$$\frac{N^*}{\phi_c N_c} + \frac{M_x^*}{\phi_b M_{bx}} \leq 1 \tag{9}$$

This approach is consistent with AS 4084 [15] which does not require a design to account for bimoments for racks in general. It is only when the rack is subjected to primary torsion action that the Standard requires bimoments to be considered.

A load factor of 1.4 is used for the pallets to determine the design loads N^* and bending moments M_x^*. The self-weight of the rack is ignored.

The Direct Strength Method [19] in Section 7 of the AS/NZS 4600 [18] is used in the present work to calculate the nominal capacities N_c and M_{bx} of the upright. Specifically, the axial capacity in compression N_c is defined as the lesser of the axial global, local and distortional nominal capacities N_{ce}, N_{cl} and N_{cd}, respectively,

$$N_c = min(N_{ce}, N_{cl}, N_{cd}) \tag{10}$$

and the nominal bending moment capacity M_{bx} about the x-axis of bending is defined as the lesser of the global, local and distortional nominal moment capacities M_{bxe}, M_{bxl}, M_{bxd}, respectively,

$$M_{bx} = min(M_{bxe}, M_{bxl}, M_{bxl}) \tag{11}$$

The global nominal capacity M_{bxe} is a function of the bending moment distribution in the upright through the elastic buckling moment M_o,

$$M_o = C_b A_u r_{ol} \sqrt{f_{oy} f_{oz}} \tag{12}$$

where C_b is a coefficient depending on moment distribution in the unbraced segment of the upright, A_u is the gross cross-sectional area, r_{ol} is the polar radius of gyration about the shear centre and f_{oy} and f_{oz} are the elastic buckling stresses for flexural buckling about the y-axes (perpendicular to the symmetry axis) and torsional buckling, respectively.

Detailed rules to determine N_{ce}, N_{cl}, N_{cd}, M_{bxe}, M_{bxl}, M_{bxd} are given in [8, 18].

4.3.1 Effective buckling lengths

For the calculation of N_{ce}, the Australian Standard AS 4084 [15] recommends effective lengths l_{ey} and l_{ez} for buckling about the y- (down-aisle) and z- (torsional) axes equal to and 0.7 times the upright frame bracing pitch, respectively. These effective lengths are for buckling in the plane of the upright frames. Consistent with [12], the rail beams are not considered to form part of the upright frame and ignored in the calculation of the frame bracing pitch. The upright frame bracing pitches (h and h_p) are defined in [15] and shown in Figure 18. These values are adopted in the present work, although there are peculiarities associated with this 2D approach [20].

Also, as per [15], for each member of the simple upright model, the effective length l_{ex} for buckling about the x-axis (in the down-aisle plane) is calculated as

$$l_{ex} = \pi \sqrt{\frac{EI_x}{N_{crb}}} \tag{13}$$

where I_x is the second moment of area about the x axis, and N_{crb} is the elastic buckling load of the upright determined from a rational frame buckling analysis.

The structural model used in the rational frame buckling analysis for each of Models A, B and C is exemplified in Figure 19. It should be noted that the horizontal translational restraints at the two pallet levels do not represent actual physical restraints, whether rigid or partial (due to pallet base friction, for example). That is, horizontal translational restraints are applied wherever pallets are present, irrespective of whether friction is ignored or considered in the design. The horizontal translational restraints applied where pallets are present are "notional", and reflect the fact that notional horizontal loads, i.e. out-of-plumb loads, have been applied there in conjunction with second-order analysis to account for the bending moment amplifications in the upright, and is consistent with the use of an effective flexural length determined from Eq. (13) in the member design check.

5 RESULTS

5.1 Effects of pallet restraint

In this study, two values for the frame bracing pitches (with $h = h_p$ in Figure 18), being 1,500 mm and 2,000 mm, are considered.

5.1.1 Frame bracing pitch h = 1,500 mm

Figure 20 plots the ratios of the maximum member action-to-capacity ratio, calculated using Eq. (9), of Model C (current industry practice) to that of Model A, and to that of Model B, for the 36 racks given in Table 1 having a frame bracing pitch $h = h_p$ of 1500 mm. Detailed results can be found in [8]. A ratio greater than 1.0 in Figure 20 indicates that the current industry practice results in uneconomical designs.

Figure 20 shows that for 12 racks out of 36, incorporating the horizontal restraining effect provided by the pallets would provide more economical designs than current industry practice, with a decrease in the member action-to-capacity ratio of up to 6% (Rack 1). On average for the 12 racks, the decrease is 2%.

For the remaining 24 racks, ignoring the pallet restraints would lead to less conservative designs, with an increase in the member action-to-capacity ratio of up to 7% (Rack 30). On average for the 24 racks, ignoring the pallet restraints increases the design capacity by 3%. This counterintuitive result is due to the role of the pallet restraints in increasing the design bending moment of the upright under the critical load case. While considering the pallet restraints resulted in larger bending moments at the upright bases, it resulted in smaller maximum bending moments at the critical sections (which are usually between the floor and the first rail beam elevation for the critical load case illustrated in Figure 12). Figure 21 shows the bending moment distribution in the upright for Models A and C, and the coefficient C_b in Eq. (12), for the critical load case for Rack 25. It can be seen that ignoring the pallet restraints leads to a design bending moment in the critical upright of 1326 kN.mm, that is 12% less than the design bending moment of 1502 kN.mm when considering pallet restraints, but with similar C_b coefficient. As specified in Section 4.3.1, it should be noted that second-order bending moments have been accounted for in the analysis, and the effective lengths used in the member design checks are not affected by the pallet restraints.

Table 2 summarises the average maximum member action-to-capacity ratios given in Figure 20.

5.1.2 Frame bracing pitch h = 2,000 mm

Figure 22 plots the ratios of the maximum member action-to-capacity ratio of Model C (current industry practice) to that of Model A, and to that of Model B, for the 36 racks given in Table 1 having a frame bracing pitch h of 2000 mm. Detailed results can be found in [8].

Similar conclusions to those in Section 5.1.1 can be drawn. Results show that for 11 racks out of 36, considering the horizontal restraining effect provided by the pallets would provide more economical designs than the current industry practice, with a decrease in the member action-to-capacity ratio of up to 5% (Rack 1) and an average decrease of 2%. For the remaining 25 racks,

ignoring the pallet restraints leads to less conservative designs, with a maximum increase in the member action-to-capacity ratio of 5% (Rack 25) and an average increase of 3%. Table 2 summarises the average maximum member action-to-capacity ratios given in Figure 22.

5.1.3 Critical load cases

When the pallet restraints are considered in the analysis (Models A and B), the load case involving the loading scenario illustrated in Figure 12, which corresponds to a fully loaded rack except for one compartment at the first rail beam elevation, is found to generally govern the design. However, for the 4-storey drive-in racks numbers 26 and 30, the load case shown in Figure 23 (a) is found to provide an action-to-capacity ratio of up to 13% higher than the load case involving the loading scenario shown in Figure 12. Despite the fact that a lower axial load occurred in the critical upright, the loading scenario induces a buckling length l_{ex} about twice that for the loading scenario shown in Figure 13, and therefore leads to a reduced axial capacity.

When the pallet restraints are ignored in the analysis, the load case involving the loading scenario shown in Figure 12 is also found to generally govern the design. However, the load cases shown in Figure 23 (b) for the 4-storey drive-in rack number 4, Figure 23 (c) for the 5-storey rack number 21 and Figure 23 (d) for the 6-storey drive-in racks numbers 21, 22 and 36 govern the design with action-to-capacity ratios of 2%, 3% and 4.5% higher than those for the loading scenario shown in Figure 12, respectively.

In view of the above results, for ULS design ignoring pallet bracing effects, limiting the analysis to the load case involving the loading scenario shown in Figure 12 and a fully loaded rack, would only induce a limited error in the action-to-capacity ratio and may be considered to be “sufficient for considering the pattern load effects” as stated in [12].

5.2 Required friction

The minimum friction coefficient μ needed to prevent the pallets from sliding on the rail beams is investigated herein for Model A. The friction forces S_f developing between the pallets and the rail beams are extracted from the horizontal reactions at each loaded rail beam elevation of the single upright model. The friction effect s is then calculated as,

$$s = \frac{S_f}{W} \tag{14}$$

where W is the axial load applied by the pallets to the upright at the rail beam elevation.

Figure 24 shows the friction effect s for all loading cases and for the 36 drive-in racks defined in Table 1. All values in Figure 24 are less than the design static friction coefficient of 0.439 recommended by Hua and Rasmussen [3] (see Section 1), indicating that, under normal operating conditions, sliding is unlikely to occur between the pallets and the rail beams, and that pallet bracing restraints could be considered in the design of drive-in racks. Moreover, the friction effect s is dependent on the number of storeys (or rail beam elevations), as seen in Figure 24. The more storeys for a given rack height, the greater the friction effect and hence the more likely the pallets are to slide. Results show that, for a given number of storeys, the friction effect decreases approximately linearly with the height of the rack.

6 CONCLUSIONS

This paper analyses the influence of horizontal bracing restraints provided by the pallets on the behaviour and design of steel drive-in racks. The pallets are shown to significantly influence the bending moment distribution in the uprights. The single upright model presented by Godley was improved by including the restraints provided by the rail beams and the pallets. Comparison with advanced 3D Finite Element Analyses showed that the improved single upright model was able to accurately reproduce the bending moment distribution in the upright in the down-aisle direction under gravity and out-of plumb loads.

Using the improved single upright model, analyses were run for 36 drive-in rack configurations. All possible loading cases were analysed. Results showed that ignoring the pallet restraints in the design usually leads to design bending moments in the critical upright less than the design bending moments obtained when considering pallet restraints. Specifically, ignoring the pallet bracing effects in design, as in the current industry practice, was shown to lead to a less conservative design with an action-to-capacity ratio for the critical upright being reduced in the order of 4%.

The standard load case involving a fully loaded rack except for one compartment at the first rail beam elevation was found to govern the ultimate limit state design of most racks. However, other loading scenarios were found to govern the design of some drive-in racks having 4 to 6 storeys, with action-to-capacity ratios up to 5% greater than those produced by the standard load case.

Results show that under normal operating conditions, the friction coefficient between the pallets and the rail beams is sufficient to prevent sliding of the pallets, and therefore the effect of pallets could be considered in the design of drive-in racks. However, as demonstrated in the paper, overall there is no benefit to the be gained from including the effect of pallet restraint in the design.

7 REFERENCES

[1] B.P. Gilbert, K.J.R. Rasmussen "Drive-in steel storage racks I: Stiffness test and 3D load transfer mechanisms", *ASCE Journal of Structural Engineering*, 138, 135-147, 2012.
[2] M.A. Salmon, R.E. Welch, A. Longinow, "Analysis of drive-in and drive-thru storage racks", *Proceedings of the 2nd Specialty Conference on Cold-Formed Steel Structures* (Ed.: W.W. Yu), St Louis, Missouri, U.S.A., 617-639, 1973.
[3] V. Hua, K.J.R. Rasmussen, Static friction coefficient between pallets and beam rails and pallet shear stiffness tests, Research Report 914, School of Civil Engineering, The University of Sydney, Australia, 2010.
[4] B.P. Gilbert, K.J.R. Rasmussen "Impact tests and parametric impact studies on drive-in steel storage racks", *Engineering Structures*, 33, 1410-1422, 2011.
[5] B.P. Gilbert, K.J.R. Rasmussen "Determination of accidental forklift truck impact forces on drive-in steel storage rack structures", *Engineering Structures*, 33, 1403-1409, 2011.
[6] M.H.R. Godley, "The behaviour of drive-in storage structures", *Proceedings of the 16th International Specialty Conference on Cold-Formed Steel Structures* (Eds.: R.A. LaBoule, W.W. Yu), Orlando, Florida, U.S.A., 340-352, 2002.
[7] B.P. Gilbert, K.J.R. Rasmussen, Finite Element modelling of steel drive-in rack structures, Research Report R901, School of Civil Engineering, The University of Sydney, Australia, 2009.
[8] B.P. Gilbert, L.H. Teh, R.X. Badet, K.J.R. Rasmussen, Determination of the influence of the pallets on the design of drive-in steel storage racks, Research Report CIEM/2013/R04, Centre for Infrastructure Engineering and Management, Griffith University, Australia, 2013.
[9] M.H.R. Godley, R.G. Beale, X. Feng, "Rotational stiffness of semi-rigid baseplates", *Proceedings of the 14th International Specialty Conference on Cold-Formed Steel Structures* (Eds.: W.W. Yu, R.A. LaBoule), St Louis, Missouri, U.S.A., 323-335, 1998.
[10] Abaqus, *Abaqus ver. 6.10 - User manual*, (ABAQUS, Inc.), Providence, U.S.A., 2010.
[11] Strand7, *Using Strand7 - User manual - Release 2.4.4*, (G+D Computing Pty Ltd), Sydney, Australia, 2010.
[12] FEM 10.2.07, *The Design of 'Drive-in' and 'Drive-through' pallet racking*, Federation Europeenne de la Manutention, Brussels, Belgium, 2012.
[13] B.P. Gilbert, *The behaviour of steel drive-in racks under static and forklift truck impact forces*, PhD Thesis, School of Civil Engineering, The University of Sydney, Sydney, Australia, 2010.
[14] B.P. Gilbert, K.J.R. Rasmussen "Determination of the base plate stiffness and strength of steel storage racks", *Journal of Constructional Steel Research*, 67, 1031-1041, 2011.
[15] AS 4084, *Steel storage racking*, Standards Australia, Sydney, Australia, 2012.
[16] EN 15512, *Steel static storage systems - Adjustable pallet racking systems - Principles for structural design*, European Committee for Standardization (CEN), Brussels, Belgium, 2009.

[17] RMI, *Specification for the design, testing and utilization of industrial steel storage racks*, Rack Manufacturers Institute, Charlotte, U.S.A., 2008.
[18] AS/NZS 4600, *Cold-formed steel structures*, Standards Australia, Sydney, Australia, 2005.
[19] B.W. Schafer, "Designing cold-formed steel using the direct strength method", *Proceedings of the 18th International Specialty Conference on Cold-Formed Steel Structures* (Eds.: R.A. LaBoule, W.W. Yu), Orlando, Florida, 475-490, 2006.
[20] L.H. Teh, G.J. Hancock, M.J. Clarke "Analysis and design of double-sided high-rise steel pallet rack frames", *ASCE Journal of Structural Engineering*, 130, 1011-1021, 2004.

Rack n°	Height (mm)	Nb stories	Design pallet load (kg)	Upright		
				type	width (mm)	thk. (mm)
1	3775	2	950	SD	70	1.2
2		3	950	SD	90	1.5
3			1210	RF	90	1.2
4		4	690	RF	90	1.2
5	5025	2	950	SD	90	1.2
6			1210	SD	90	1.2
7		3	690	RF	90	1.2
8			950	RF	90	1.2
9			1210	RF	90	1.5
10		4	950	SD	110	1.5
11			1210	RF	110	1.5
12			1470	RF	125	1.5
13	6275	2	1470	RF	90	1.2
14		3	950	RF	90	1.5
15			1210	SD	110	1.5
16			1470	RF	110	1.5
17		4	430	SD	90	1.5
18			950	SD	110	1.2
19			1210	RF	110	1.9
20			1470	RF	125	1.5
21		5	950	RF	110	1.9
22		6	690	RF	110	1.5
23			950	RF	125	1.5
24	7525	3	1210	SD	110	1.5
25			1470	RF	110	1.5
26		4	430	RF	90	1.2
27			950	RF	110	1.9
28		5	950	SD	125	1.9
29	8775	3	1210	SD	125	1.5
30		4	430	RF	90	1.7
31			950	SD	125	1.9
32			1210	RF	125	1.9
33		5	950	SD	150	1.9
34			1210	RF	150	1.9
35			1470	RF	150	2.4
36		6	950	RF	150	1.9

Table 1: Rack configurations

	Model C (current practice) / Model A		Model C (current practice) / Model B	
h (mm)	Average ratio	CoV	Average ratio	CoV
1,500 mm	0.99	0.029	1.03	0.034
2,000 mm	0.99	0.026	1.04	0.016

Table 2: Ratio of the maximum member action-to-capacity ratios of Model C(current industry practice) to the Models A and B

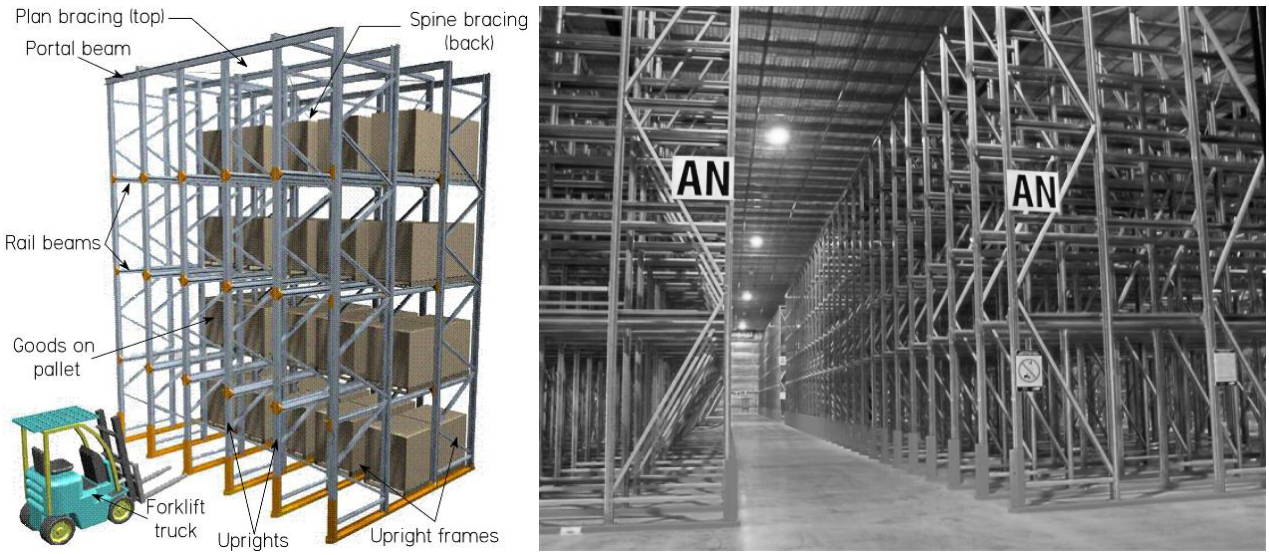

Figure 1: Example of a drive-in rack

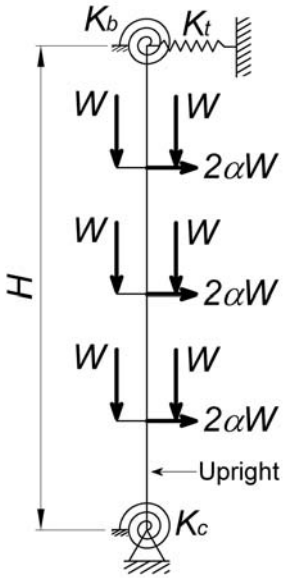

Figure 2: Drive-in rack single upright model from Godley [6]

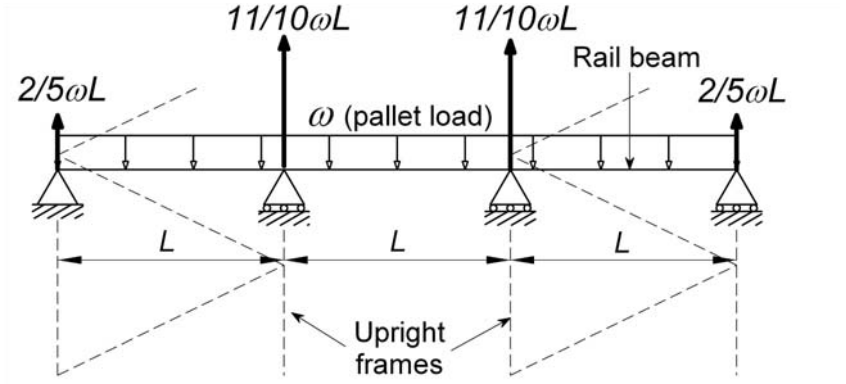

(a)

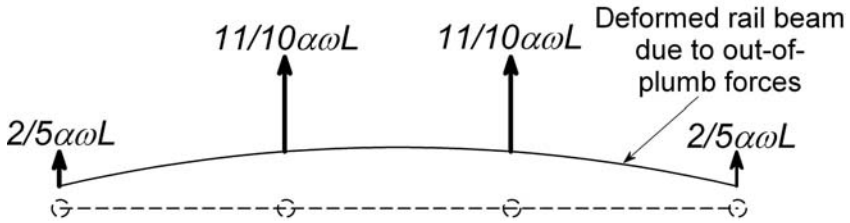

(b)

Figure 3: (a) side view of a fully loaded rail beam and resulting axial loads in the uprights and (b) top view deformed shape of the rail beam and frames under out-of-plumb forces

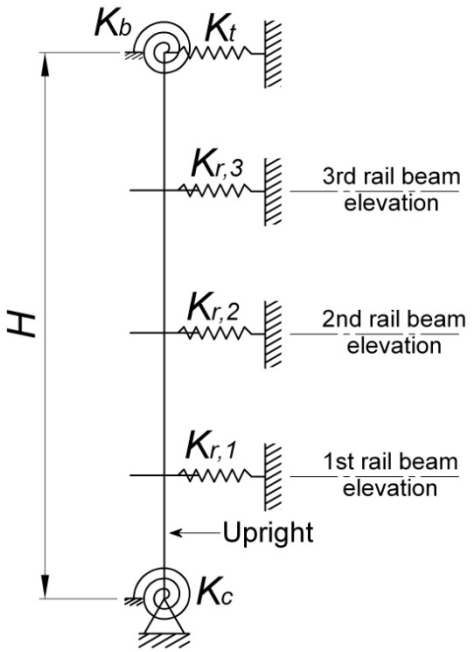

Figure 4: Single upright model with rail beam restraints for a 4 stories (3 rail beam elevations) drive-in rack

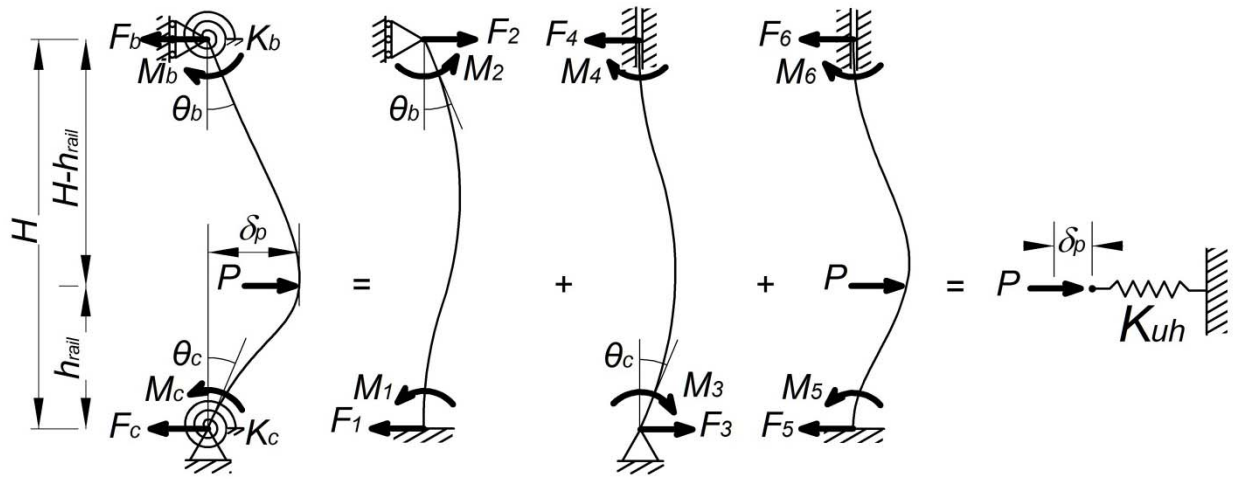

(a) (b) (c) (d) (e)

Figure 5: Upright deformation, with (a) total upright deformation, (b) bottom end fixed and top end released, (c) bottom end released and top end fixed, (d) bottom and top ends fixed with applied force P and (e) equivalent stiffness K_{uh}

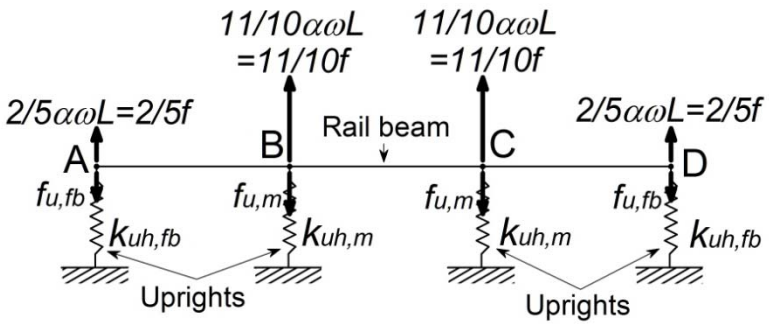

Figure 6: Model of a rail beam subjected to out-of-plumb forces

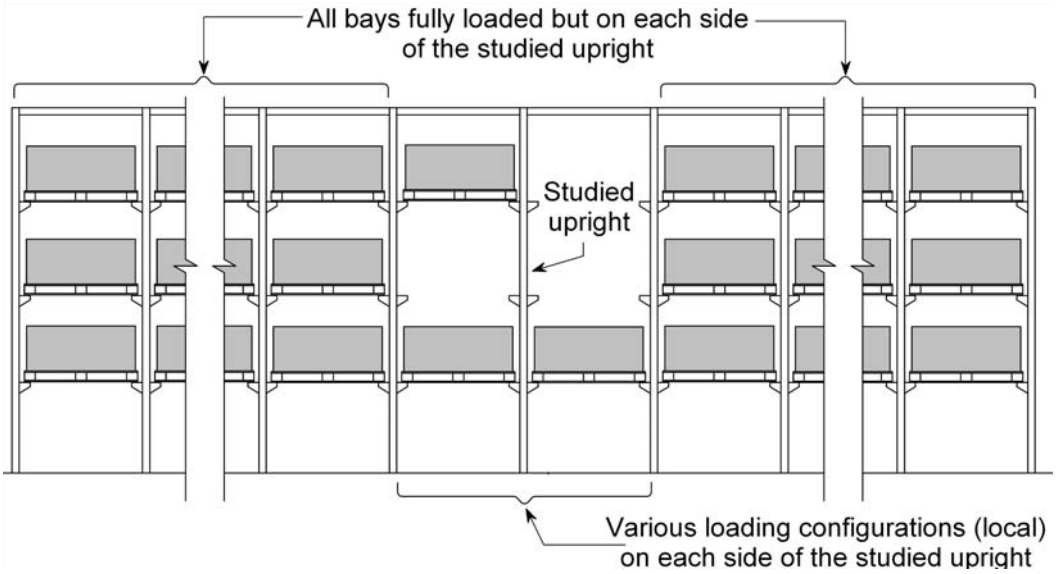

(a)

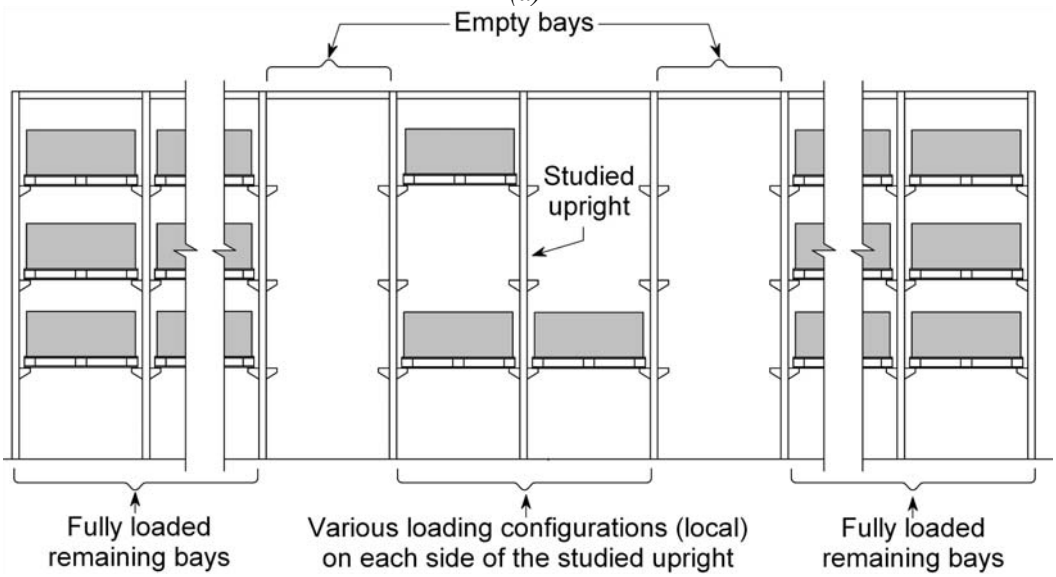

(b)

Figure 7: Studied upright for (a) Bay loading scenario A and (b) Bay loading scenario B

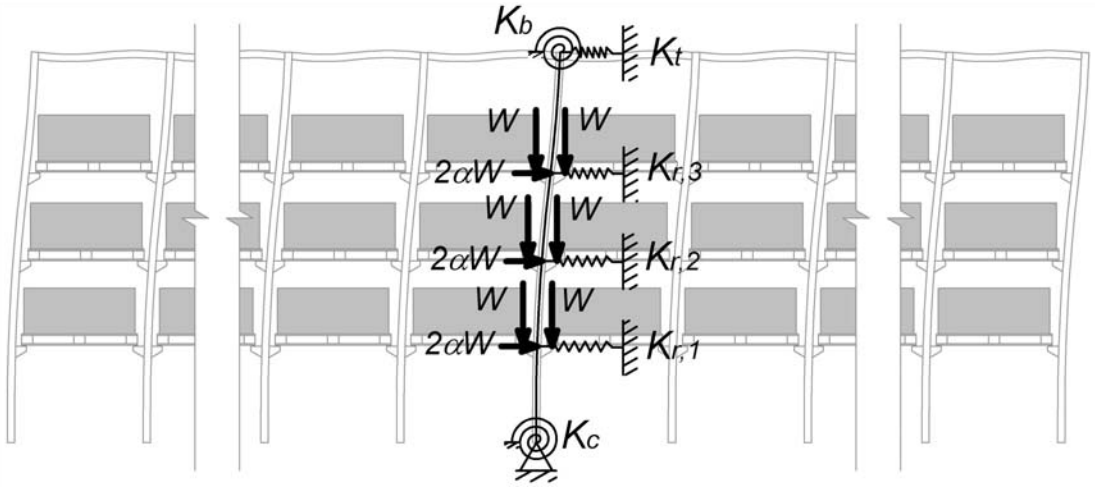

Figure 8: Deformed shape of the single upright model for a fully loaded rack

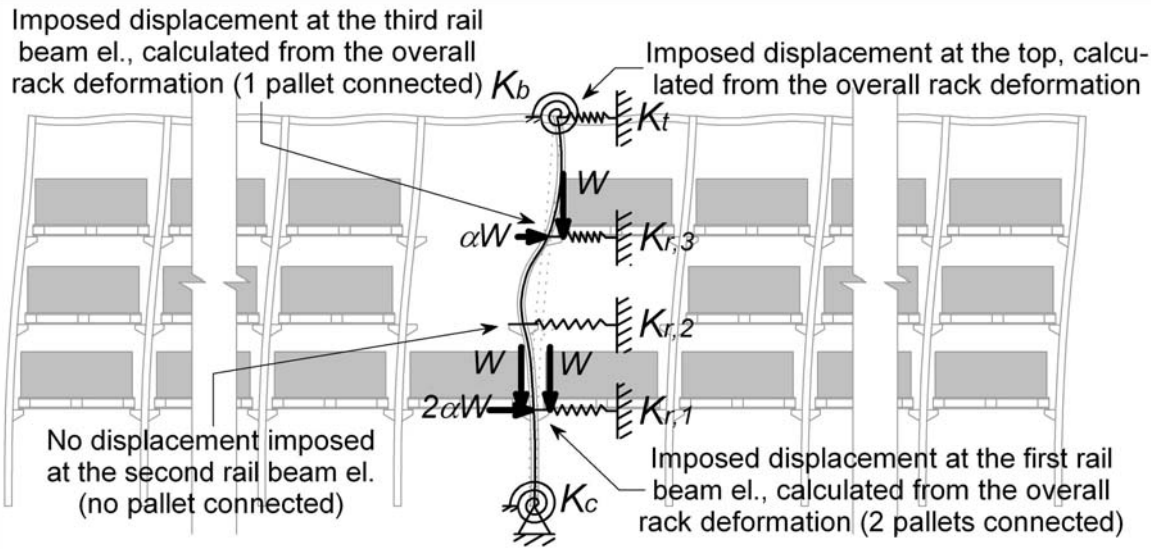

Figure 9: Improved single upright model for Bay loading scenario A (Model A)

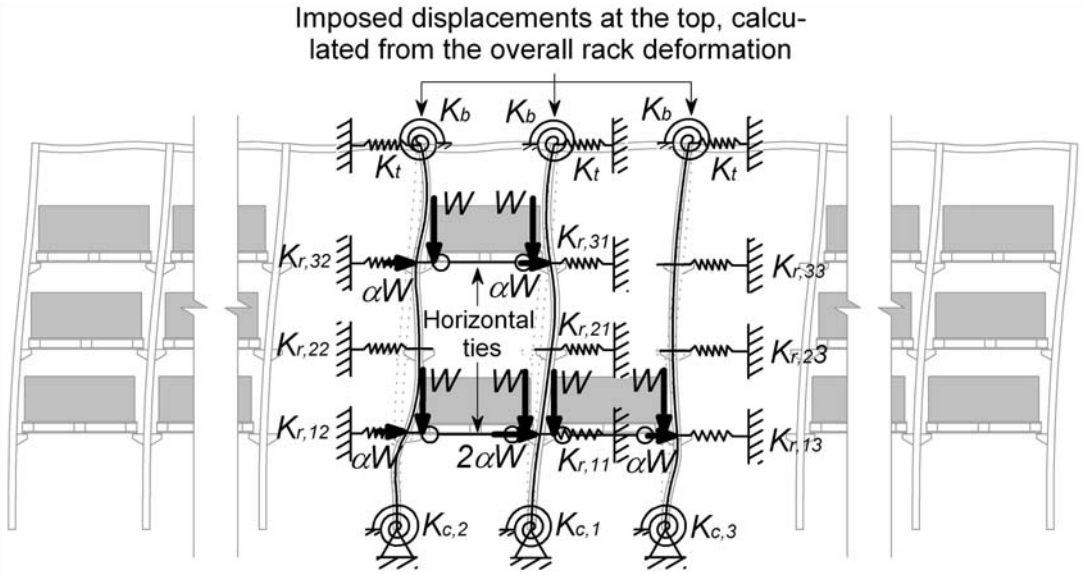

Figure 10: Improved single upright model for Bay loading scenario B (Model B)

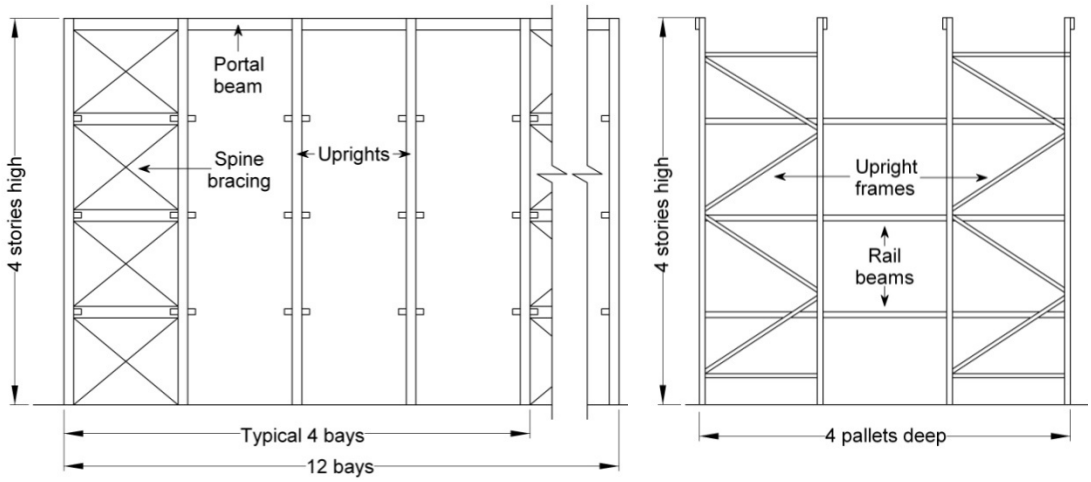

(a) – Side view (Down-aisle) *(b) – Side view (Cross-aisle)*

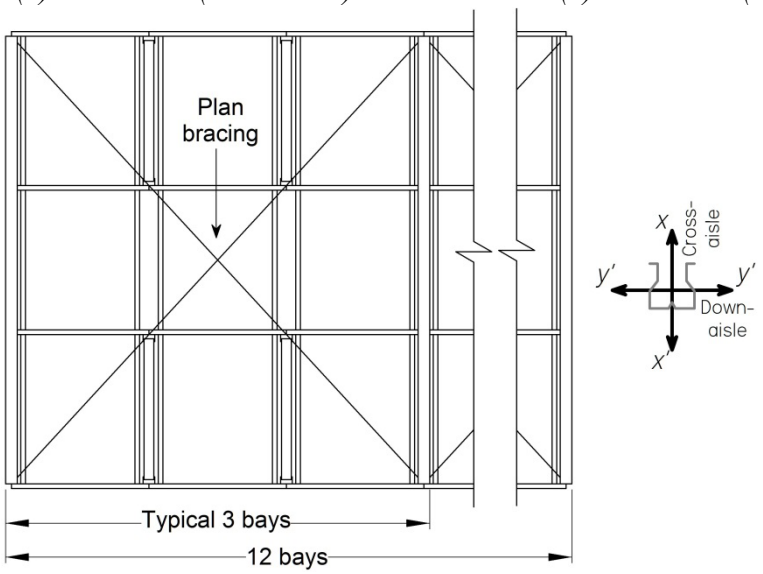

(c) – Top view

Figure 11: Case study rack

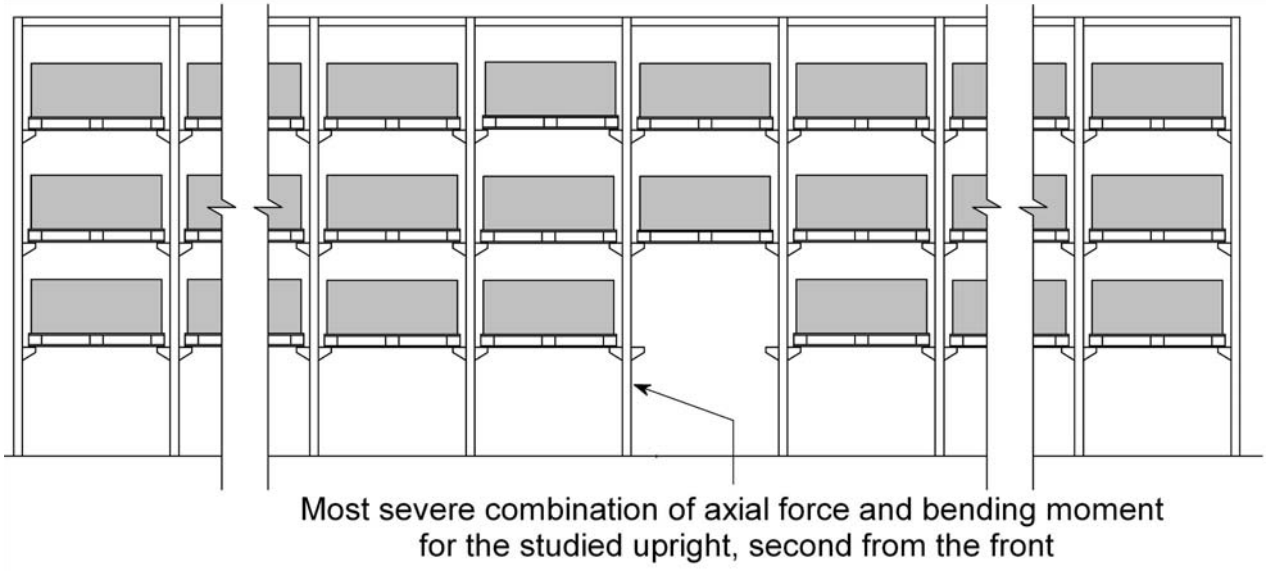

Figure 12: Loading scenario believed to generally govern the design

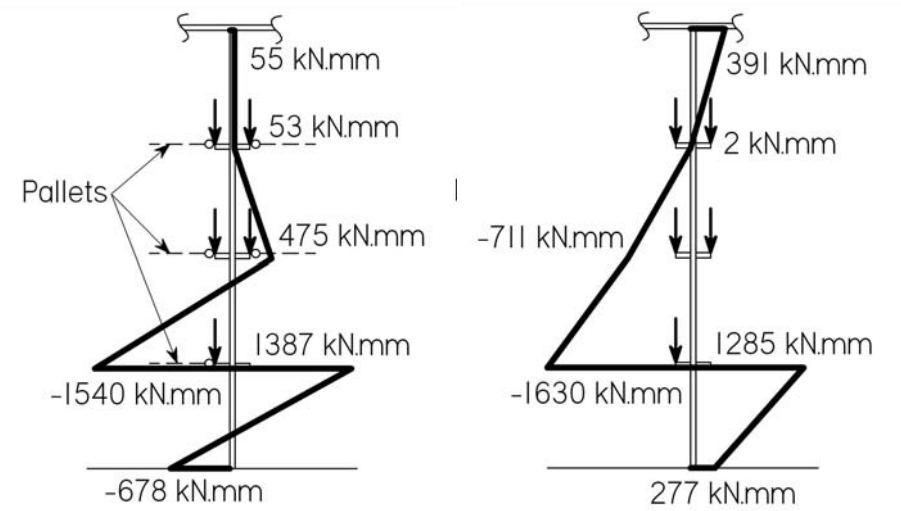

(a) *(b)*

Figure 13: Bending moment distribution in the critical upright under vertical and out-of-plumb loads for the loading scenario shown in Figure 12 using 3D advanced analysis for (a) pallets considered and (b) pallets ignored

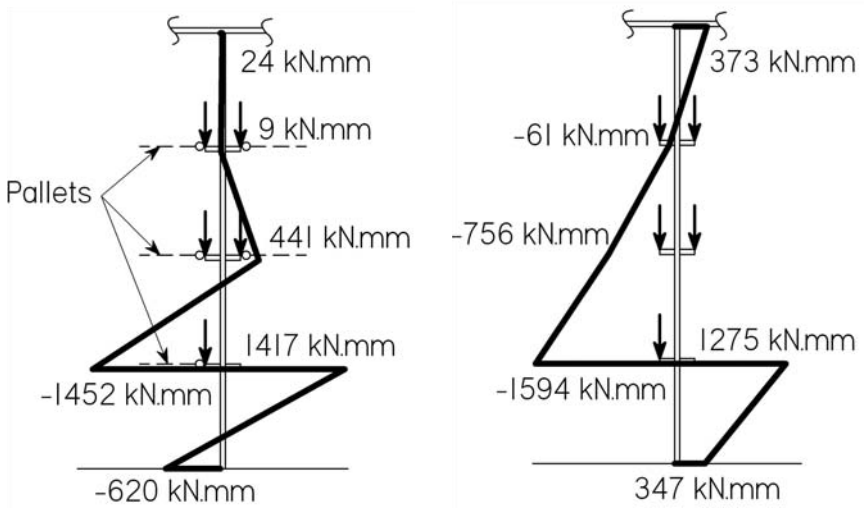

(a) *(b)*

Figure 14: Bending moment distribution in the critical upright under vertical and out-of-plumb loads for the loading scenario shown in Figure 12 using 2D analyses for (a) pallets considered and (b) pallets ignored

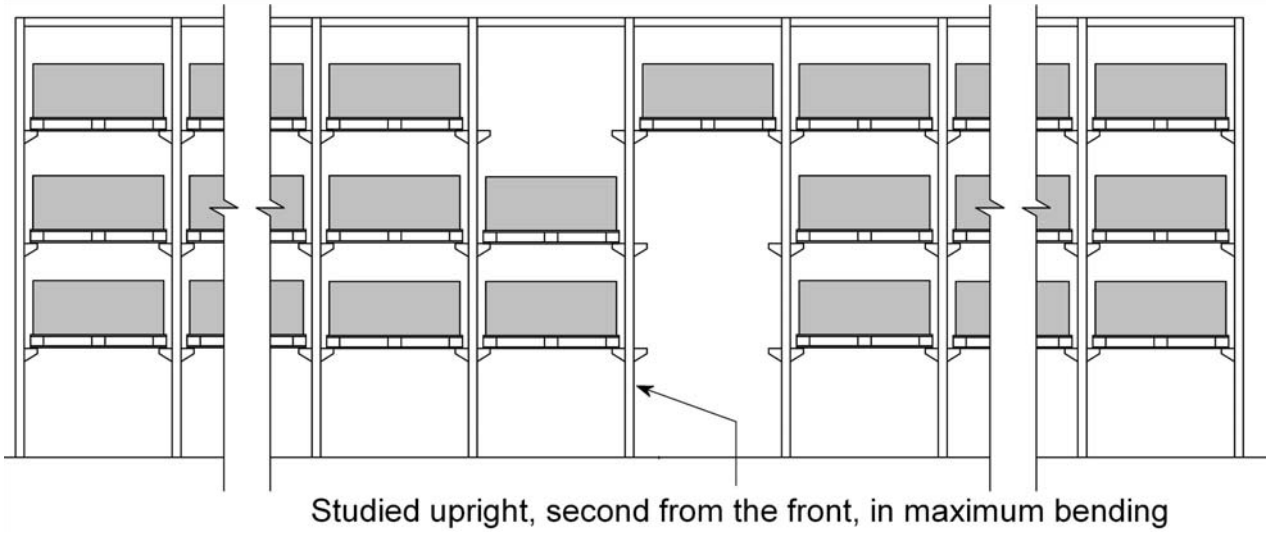

Figure 15: Loading scenario inducing maximum bending moment in a row of uprights

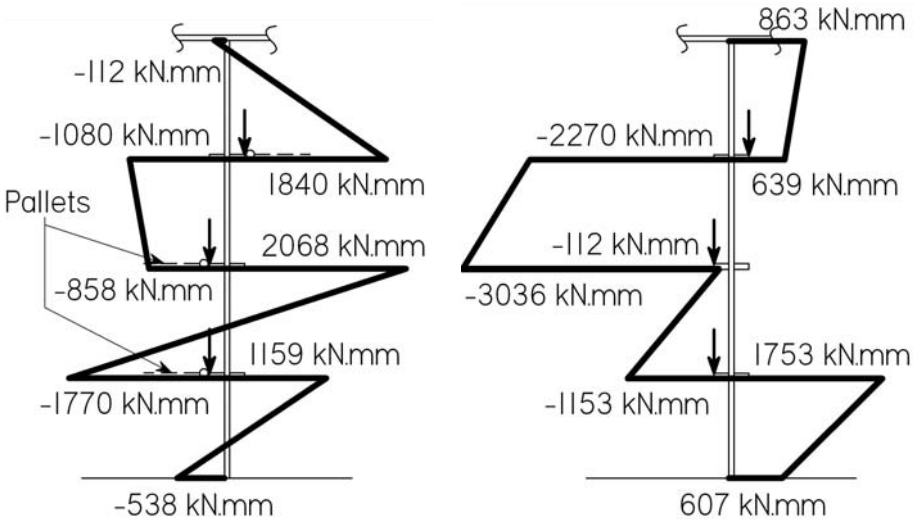

(a) *(b)*

Figure 16: Bending moment distribution in the critical upright under vertical and out-of-plumb loads for the loading scenario shown in Figure 15 and 3D advanced analysis for (a) pallets considered and (b) pallets ignored

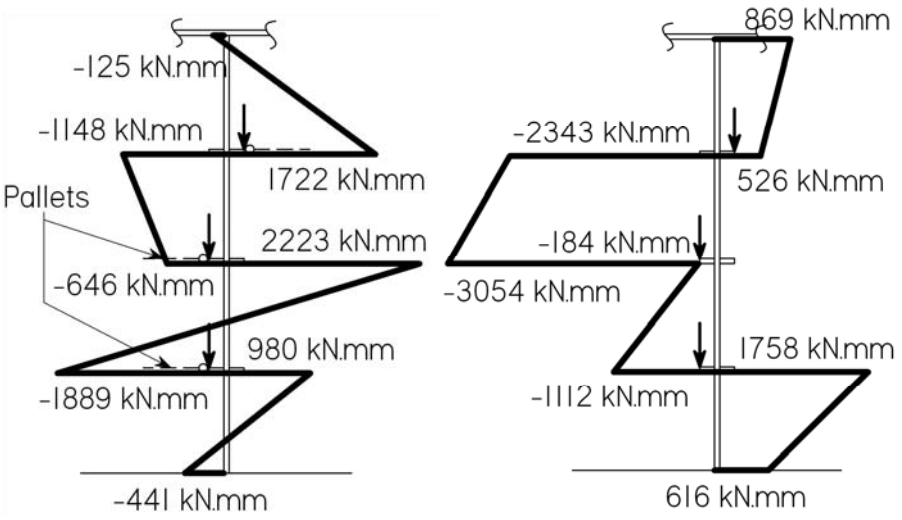

(a) *(b)*

Figure 17: Bending moment distribution in the critical upright under vertical and out-of-plumb loads for the loading scenario shown in Figure 16 and 2D analyses for (a) pallets considered and (b) pallets ignored

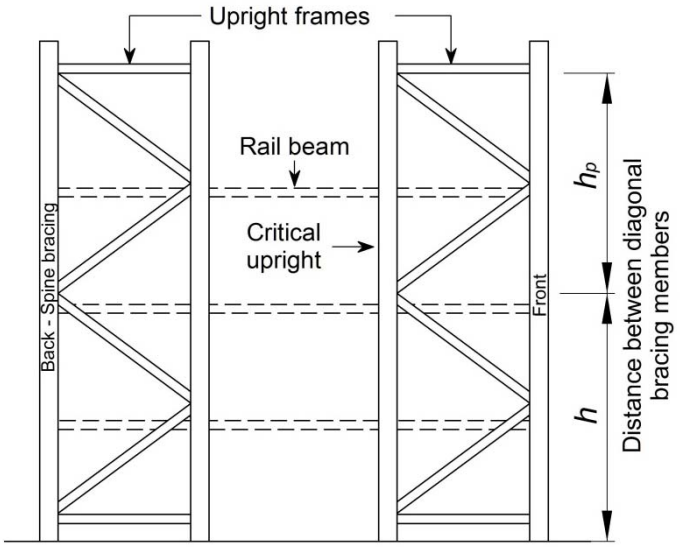

Figure 18: Frame bracing pitches h and h_p, unbraced segment

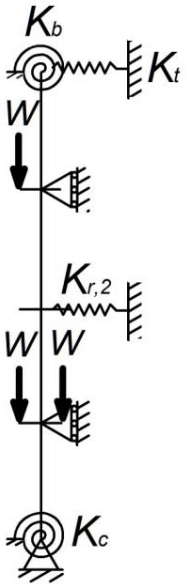

Figure 19: Example of a rack model used in the rational frame buckling analysis for each of Models A, B and C

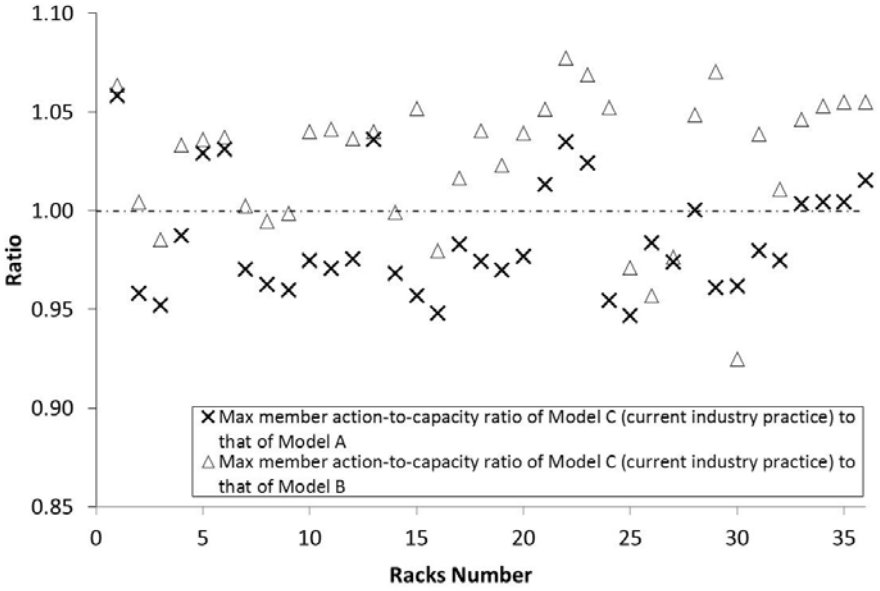

Figure 20: Influence of the horizontal pallet restraint on the action-to-capacity ratio for h = 1,500 mm

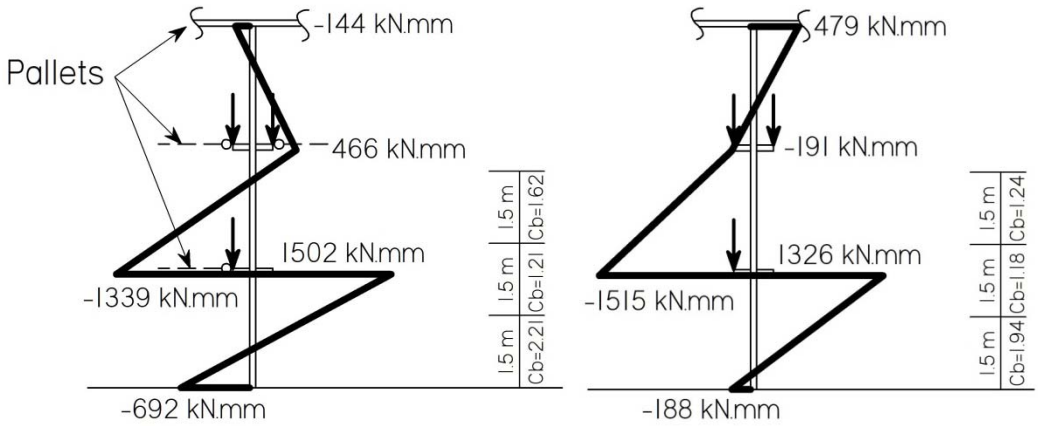

Figure 21: Bending moment distribution for the critical load case for rack 25 for (a) Model A (pallets considered) and (b) Model C (pallets ignored)

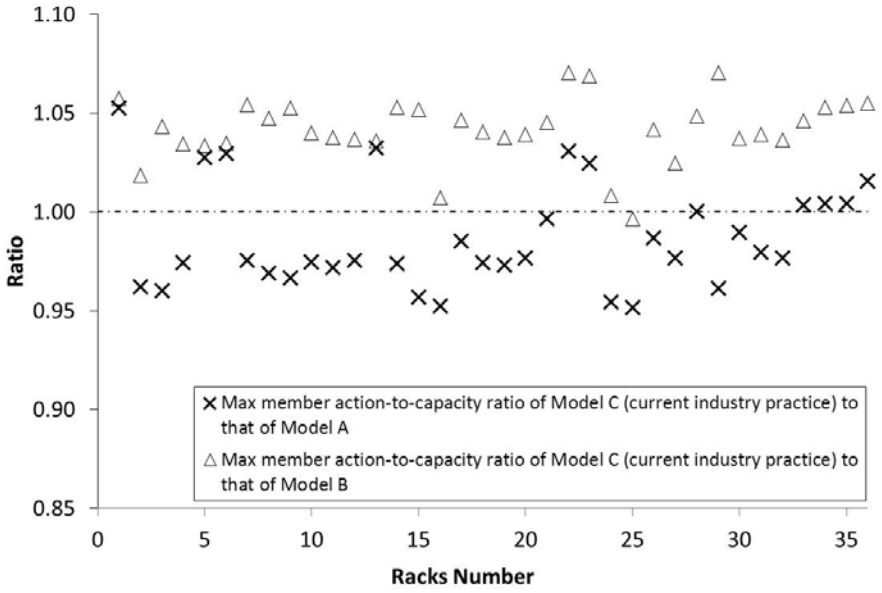

Figure 22: Influence of the horizontal pallet restraint on the action-to-capacity ratio for h = 2,000 mm

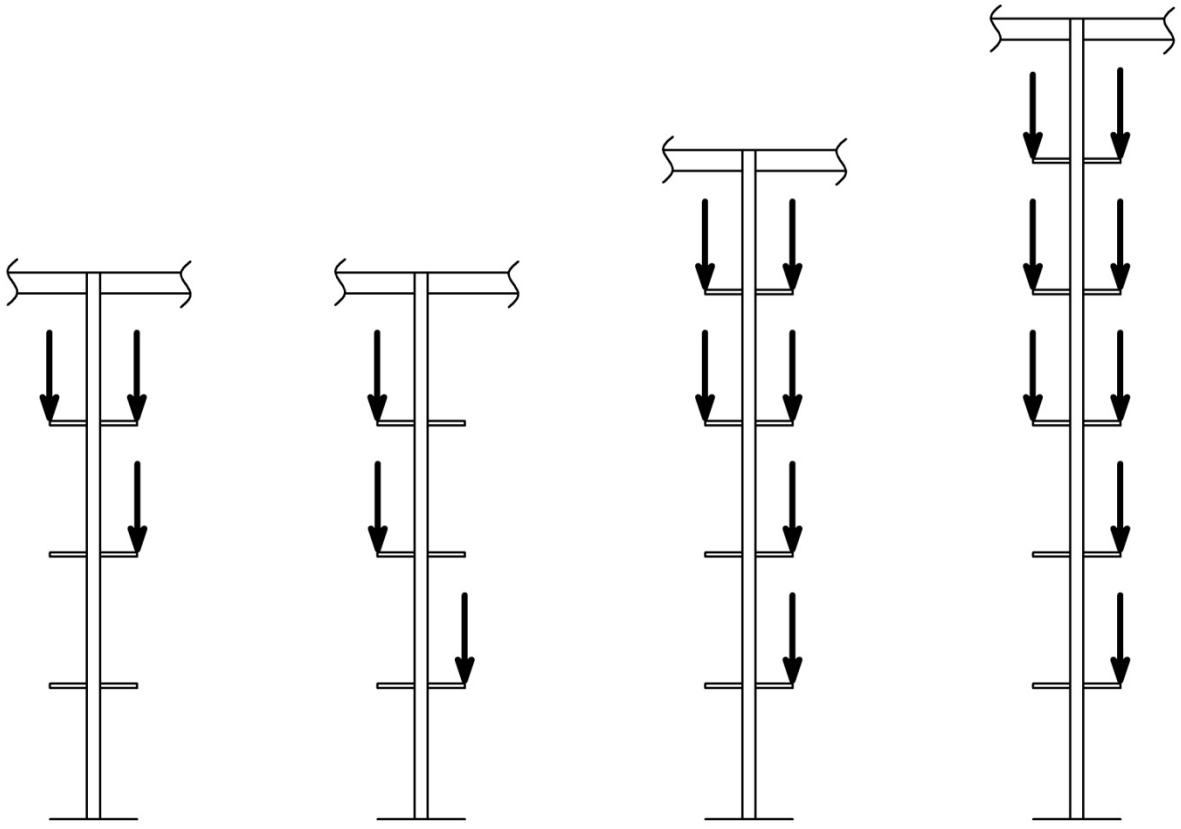

(a) *(b)* *(c)* *(d)*

Figure 23: Specific load cases governing the design

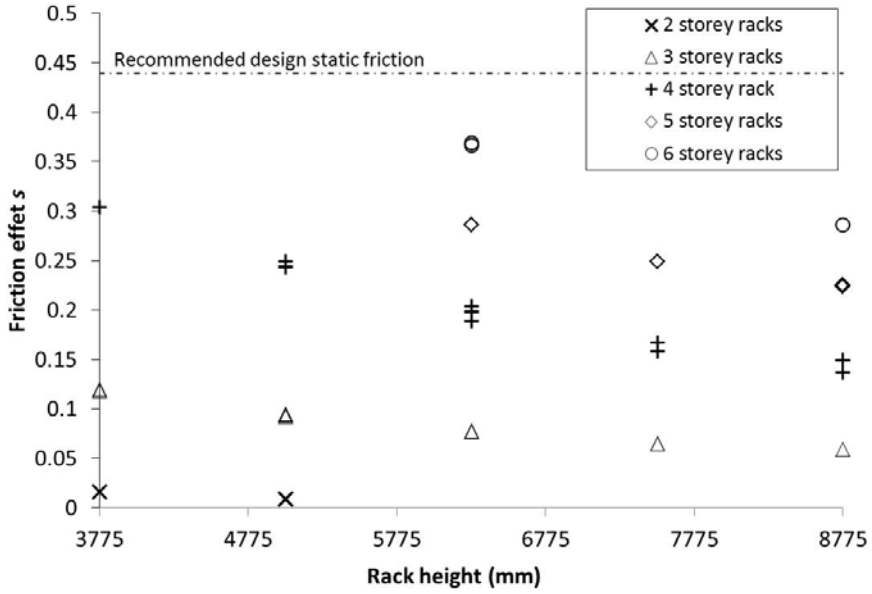

Figure 24: Friction effect s